Title

Short chain fatty acids inhibit endotoxin-induced uveitis and inflammatory responses of retinal astrocytes

Authors

Chen, Nu
Wu, Jun
Wang, Jingrui
et al.

Publication Date

2021-05-01

DOI

10.1016/j.exer.2021.108520

Peer reviewed

Experimental Eye Research 206 (2021) 108520

Contents lists available at ScienceDirect

Experimental Eye Research

journal homepage: www.elsevier.com/locate/yexer

Short chain fatty acids inhibit endotoxin-induced uveitis and inflammatory responses of retinal astrocytes

Nu Chen [a,e,3], Jun Wu [a,b,3], Jingrui Wang [a], Niloofar Piri [a,1], Feilan Chen [a,2], Tong Xiao [a], Yuan Zhao [c], Deming Sun [d], Henry J. Kaplan [a,1], Hui Shao [a,*]

[a] Department of Ophthalmology and Visual Sciences, Kentucky Lions Eye Center, University of Louisville, Louisville, KY, USA
[b] Department of Ophthalmology, Union Hospital, Tongji Medical College, Huazhong University of Science and Technology, Wuhan, PR China
[c] Department of Molecular and Cellular Biology, Sam Houston State University College of Osteopathic Medicine, Huntsville, TX, USA
[d] Doheny Eye Institute & Department. Ophthalmology, David Geffen School of Medicine/UCLA, Los Angeles, CA, USA
[e] Tianjin Key Laboratory of Retinal Functions and Diseases, Eye Institute and School of Optometry, Tianjin Medical University Eye Hospital, Tianjin, PR China

ARTICLE INFO

Keywords:
Short chain fatty acids
Intraocular inflammation
Danger signals
Retinal astrocytes
Cytokines
T cell activation

ABSTRACT

Short chain fatty acids (SCFAs) are produced by gut microbiota as fermentation products of digestion-resistant oligosaccharides and fibers. Their primary roles are functioning as major energy sources for colon cells and assisting in gut homeostasis by immunomodulation. Recent evidence suggests that they affect various organs both at cellular and molecular levels, and regulate functions in distance sites including gene expression, cell proliferation, cell differentiation, apoptosis and inflammation. In this study, we examined whether SCFAs are present in the mouse eye and whether SCFAs affect inflammatory responses of the eye and retinal astrocytes (RACs). We observed that intra-peritoneal injected SCFAs were detected in the eye and reduced intraocular inflammation induced by lipopolysaccharide (LPS). Moreover, SCFAs displayed two disparate effects on LPS-stimulated RACs – namely, cytokine and chemokine production was reduced, but the ability to activate T cells was enhanced. Our results support the existence of gut-eye cross talk and suggest that SCFAs can cross the blood-eye-barrier via the systemic circulation. If applied at high concentrations, SCFAs may reduce inflammation and impact cellular functions in the intraocular milieu.

1. Introduction

Short-chain fatty acids (SCFAs) such as acetate (C2), propionate (C3), and butyrate (C4) are solely metabolized by gut bacteria from otherwise indigestible carbohydrates, i.e., from fiber-rich diets (Sun et al., 2017). SCFA is important in not only maintaining intact gut permeability (Kim et al., 2014) but also regulation of inflammation in tissues/organs beyond the digestive system, such as lung (Theiler et al., 2019), kidney (Andrade-Oliveira et al., 2015), and brain (Matt et al., 2018). Oral SCFAs reduced mild experimental autoimmune uveitis (EAU) induced by immunization of retinal antigen and complete Freund's adjuvant (CFA) in C57BL/6J (B6) mice (Nakamura et al., 2017) confirming that SCFAs produced by gut microbiota can regulate intraocular inflammation. The reduction of immune-mediated uveitis by SCFA was partially attributed to altering migration of lymphocytes from the intestine to the eye (Nakamura et al., 2017). However, it is unknown, whether SCFAs can access the eye via the systemic circulation, execute direct effects in the eye and influence resident intraocular cells.

The eye is an immune privileged site that cannot tolerate destructive inflammatory responses without significant visual loss. However, despite immune privilege the eye remains vulnerable to both innate and adaptive immune mediated inflammation. Resident intraocular cells play an important role in the initiation and progression of intraocular inflammation following injury (Lozano et al., 2019; Slavi et al., 2018), hypoxia (Selvam et al., 2018), as well as in response to autoreactive T cells (Jiang et al., 2014), danger signals (such as cytokines) (Ke et al., 2009), and Toll-like receptor (TLR) ligands (Jiang et al., 2009, 2012). Retinal microglia, astrocytes, Müller cells, dendritic cells (DCs), and retinal

* Corresponding author.
E-mail address: h0shao01@louisville.edu (H. Shao).
[1] Present Address: Department of Ophthalmology, St. Louis University, St. Louis, MO, USA.
[2] Present Address: Chongqing Medical University, Chongqing, PR China.
[3] Both authors contributed equally to this manuscript.

https://doi.org/10.1016/j.exer.2021.108520
Received 1 December 2020; Received in revised form 7 February 2021; Accepted 15 February 2021
Available online 20 February 2021

pigment epithelial (RPE) cells are all resident intraocular cells and play a role in inflammation because they express receptors that sense signals of injury and hypoxia, and recognize pathogen/damage-associated molecular patterns (PAMPs/DAMPs).

Our previous studies on retinal astrocytes (RACs) demonstrated they are a major subset of intraocular resident cells with the ability to produce a wide variety of cytokines and chemokines. For example, RACs can produce IL-6, TNF-α and chemokines (including CXCL1, CCL2 and CCL7) in response to ligands for TLRs (Jiang et al., 2009, 2012), and cytokines IFN-γ and IL-17 from activated uveitogenic Th1 and Th17 cells (Ke et al., 2009). After exposure to TLR ligands and pro-inflammatory cytokines (Jiang et al., 2008, 2009, 2012), RACs increase their expression of MHC class II and costimulatory molecules, enhancing uveitogenic T cell activation and differentiation. RACs also release High Mobility Group Box 1 (HMGB1), an important DAMP, after direct interaction with activated uveitogenic T cells. HMGB1 is an early and critical mediator in induction of intraocular inflammation, which enhances chemokine CXCL12 release leading to chemoattraction of inflammatory cells (Jiang et al., 2014; Yun et al., 2017). Thus, RACs are involved in many ocular diseases including uveitis (Gardner et al., 2017), glaucoma (Williams et al., 2017), diabetic retinopathy (Ly et al., 2011) and age-related macular degeneration (Ramirez et al., 2001), and are an attractive therapeutic target.

In this study, we explored whether SCFAs could directly affect intraocular inflammatory responses including RACs, since they are an important regulator of intraocular inflammation.

2. Materials and methods

2.1. Animals and reagents

Pathogen-free female C57BL/6J (B6) mice, either bred in our animal facility or purchased from Jackson Laboratory, were housed and maintained in the animal facilities of the University of Louisville. We utilized the mice at 2–7 days of age for retinal astrocyte isolation and culture, and 6–8 weeks of age for uveitis experiments. All animal studies conformed to the Association for Research in Vision and Ophthalmology statement on the use of animals in Ophthalmic and Vision Research and were approved by Institutional Animal Care and Use Committee (IACUC), university of Louisville (IACUC #20765). Mouse TLR3 agonist Poly(I:C) and TLR4 agonist LPS-EK (*E. coli* K12) were obtained from Invivogen, and recombinant mouse IL-17 from R&D. SCFAs of sodium acetate (C2), propionate (C3), and butyrate (C4) were purchased from Sigma. All antibodies for flow cytometry were purchased from eBiosciences unless otherwise specified.

2.2. SCFAs assay by gas chromatography mass spectrometry (GCMS)

8-week old female B6 were intraperitoneally (ip) injected with sodium acetate $^{13}C_2$ (Sigma) at 4 mg per mouse. After 30 min, mice were euthanized and eye, brain and liver were collected, cut into small pieces, frozen immediately in liquid nitrogen and stored in 1.5 mL Eppendorf tube at −80 °C freezer. All sample processing was performed at 4 °C to minimize the loss of volatile SCFAs. After adding water at a ratio of 1 mg tissues/10 μL water, the mixture was homogenized for 20 min and then centrifuged at 4 °C and 12,000 rpm for 20 min. 200 μL supernatant of homogenized eye, brain and liver were derivatized with 80 μL 0.1M PB buffer (pH = 8.0) and 560 μL 100 mM PFBBR in acetone and incubated at 60 °C for 30 min. Samples were extracted by 200 μL hexane or 100 μL hexane. Both unlabeled and ^{13}C labeled acetic acid in the supernatants of the samples were detected in our school core center using the method which they published previously (He et al., 2018).

2.3. LPS induced uveitis and its evaluation

EIU was induced in B6 mice using a previously described protocol (De Majumdar et al., 2017). In brief, *Escherichia coli* 055:B5 LPS (Sigma) dissolved in pyrogen-free PBS was intravitreally given to the eye (250 ng/1μl/eye) using a 30-gage needle and a 10 μL syringe (Hamilton) (Rosenbaum et al., 2011). 18 h after LPS injection, eyes were examined by Leica stereo zoom microscope before and after pupil dilation using 0.5% tropicamide and 1.25% phenylephrine hydrochloride ophthalmic solutions. The severity of clinical ocular inflammation was graded according to a previously defined scoring system (Table 1) by Qiu et al. (2014).

Table 1
Criteria of EIU clinical scoring.

Clinical signs	Grade of Signs	Score
Iris hyperemia	Absent	0
	Mild	1
	Moderate	2
	Severe	3
Exudate in anterior chamber	Absent	0
	Small	1
	Large	2
Hypopyon	Absent	0
	Present	1
Pupil	Normal	0
	Miosed	1
Maximum possible score		7

Some of the eyes were collected for histological examination (Jiang et al., 2008). Some of them were dissected following the published protocol (Chu et al., 2016) for inflammatory cell analysis by flow cytometry and cytokines/chemokine detection in aqueous humor (AqH) by ELISA.

2.4. Immunofluorescence staining for histology

This procedure was performed as we previously reported (Jiang et al., 2008). In brief, paraffin-embedded tissue slides were deparaffinized and rehydrated with xylene and 100, 95, and 80% ethanol. After antigen retrieval in a citrate-buffered solution in a boiling water bath, the tissue was blocked by incubation with 3% BSA for 1 h at room temperature, then the slides were stained with Alexa Fluor 488 conjugated monoclonal Ab (mAb) against glial fibrillary acidic protein (GFAP) (1:50, eBioscience). After mounting with blue DAPI, the sections were viewed on a laser scanning confocal microscope (Olympus, FV3000). The photos representative of a single plane were taken under the same image acquisition parameters (laser gain, laser power, offset etc.) and analyzed using Fluoview software.

2.5. Western blot for GFAP expression

The retinas were extracted from the eyes of naïve, LPS and LPS plus C4-treated mice and washed thoroughly in cold PBS. Retina tissues were homogenized and lysed with cold RIPA buffer including protease inhibitors (Thermo) for 30 min on ice and then centrifuged at 12,000 g for 15 min at 4 °C. The supernatants were collected for determining protein concentrations using a Pierce BCA protein assay kit (Thermo), aliquoted and stored at −80 °C for further analysis. A total of 15 μg protein samples were electrophoresed on 10% or 12% SDS-PAGE gels and transferred onto PVDF membranes (Sigma). The blotting was performed using the "Mini PROTEAN Tetra Electrophoresis System" (Bio-Rad) for 1.5 h at 85 V. Afterwards, the protein transferred membranes were blocked with 5% non-fat milk in Tris-buffered saline (TBST, pH 7.4) for 1 h at room temperature (RT), and then incubated overnight at 4 °C with different primary antibodies. Antibodies for β-actin (1:5000) and GFAP (1:2000) were purchased from Cell Signaling Technology and Millipore, respectively. After washing with TBST for 3 times, membranes were incubated with secondary goat anti-rabbit or anti-mouse antibodies (Santa Cruz) for 1 h at RT, followed with washing for 3 more times. The blots were visualized using an enhanced chemiluminescence detection

A

	Peak area of ^{13}C labeled C2	Peak area of unlabeled C2	% of ^{13}C labeled C2/unlabeled C2
Blank	0	4437.7±1134	0
Eye	1113.7±342.4	40445.3±11977.1	2.75±0.15***
Brain	902.3±186.1	171964.3±129333.3	0.68±0.32
Liver	409.3±222	57108±32817.9	0.72±0.34

***: p<0.001 compared to brain and liver

B

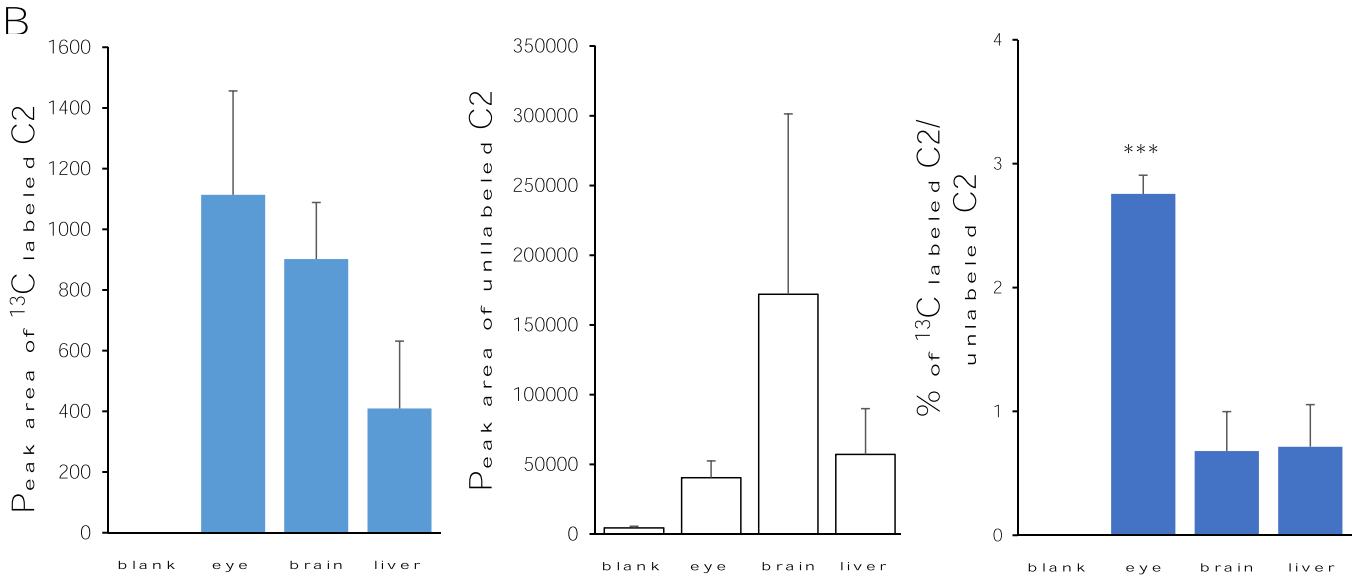

Fig. 1. *Both unlabeled and ^{13}C labeled sodium acetate (C2) were detected in the eyes.*
B6 mice were ip injected with 4mg/mouse of ^{13}C isotopomer labeled precursor of C2. Eyes, brain and liver were collected after 30 min and analyzed by gas chromatography mass spectrometry (GCMS). Peak area of ^{13}C2 and unlabeled C2 of the blank, eye, liver and standard samples from mice were summarized in table (A) and in the Bar graph (B). Data are mean ± SD of 3 mice with 2 repeats and analyzed by one-way ANOVA.

kit (Millipore). All bands were quantified using ImageJ software, and the band densities were normalized with respect to the β-actin values.

2.6. Culture of mouse retinal astrocytes

The isolation and culture of mouse RACs have been reported previously (Jiang et al., 2008, 2012) and modified. Briefly, eyes from B6 mice (ages of 2–7 days) were collected and single retinal neuronal cells were incubated for two weeks on poly-D-lysine–coated six-well plates, with the plates shaken for 2 h at room temperature. The supernatant, containing floating dead cells and possible microglia, was discarded and a low concentration (0.05%) of EDTA trypsin added to adherent cells with additional shaking for 40 min. The cells removed by the low concentration of EDTA trypsin were collected and transferred to a new flask. The detached cells (astrocytes) were collected and spin at 180×*g* for 5 min and then stained with Alexa Fluor 488 conjugated mAb against GFAP followed by flow cytometry analysis. For GFAP (an intracellular molecule) staining, before antibody incubation, the cells were fixed and permeabilized using a kit (Cytofix/Cytoperm Plus; BD PharMingen) according to the manufacturer's protocol. >95% GFAP positive cells will be used for experiments and cells cultured for 3–5 passages were used in experiments.

2.7. Cell cytotoxicity assay

RACs were treated with 10 mM of sodium acetate (C2), propionate (C3) and butyrate (C4) alone or in the combination of different doses of butyrate with 0.1 μg/ml of LPS for 6, 24, and 48 h. Positive control was 1% of Triton-X treated RACs, which led to 100% cell death (Li et al., 2018a). After treatments, supernatants were transferred into a new 96-well plate, cytotoxicity was determined using a standard measurement of lactate dehydrogenase (LDH) activity assay kit (Sigma). The results were quantified by a microplate reader (Molecular devise) at optical density (OD) 450 nm.

2.8. RAC culture and characterization for cytokine/chemokine production by ELISA and cell surface molecules by flow cytometry

The RACs in 12 or 24 well plates were cultured till 90% confluence and then treated with medium or C2, C3, C4 (1, 5, 10 mM) for 30 min followed by stimulation with LPS, Poly IC and IL-17 (all at the concentrations of 0.1 μg/ml). After 20 h, the culture supernatants were collected for cytokine assays of IL-6, TNF-α, CXCL1 and CXCL12 by ELISA (R&D). For surface expression of MHC class II and costimulatory molecules, RACs were cultured with LPS in the absence or presence of SCFAs as above for 48 h. The cells were then trypsinized, collected and incubated for 45 min at 4 °C in staining buffer (PBS containing 3% FCS and 0.1% sodium azide) containing isotype-matched control IgG or fluorescence-conjugated antibodies against mouse MHC class II molecules, CD80, CD86, ICOSL or CD40. The cells were then washed, resuspended in staining buffer, and analyzed by flow cytometry (FACSCalibur; BD Biosciences) using appropriate software (CellQuest; BD Biosciences).

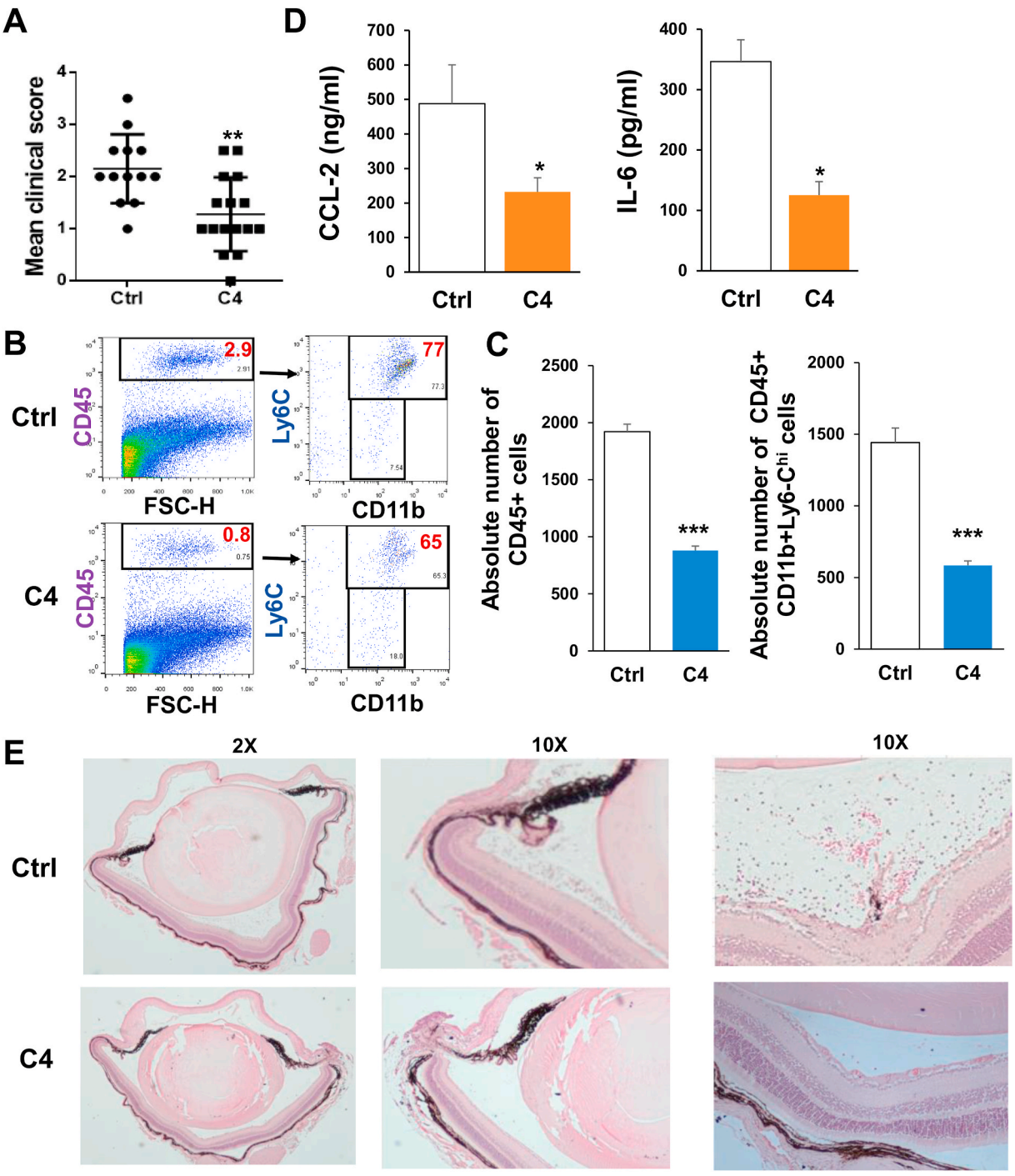

Fig. 2. *Injection of B6 mice with butyrate (C4) reduced EIU.*
B6 mice were randomly separated into two groups for ip injection of 100 μl water (control), or 500 mg/kg of C4 in 100 μl water. After 30 min, all eyes were intravitreously given 250 ng/ul of LPS. Following LPS, eyes were evaluated 18 h later. *A.* Clinical score of each group; **p = 0.004 compared to the control group using the Mann-Whitney *U* test. The data reflect two combined experiments with 13–16 eyes per group. *B–C.* A representative image (B) and absolute numbers (C) of flow cytometry analysis of $CD45^+$ leukocyte infiltration and their compositions of $CD45^+CD11b^+Ly6C^{hi}$ (monocytes/macrophages). 4–6 eyes per group were pooled for one experiment. Data from two independent experiments; means ± SEM are shown. ***$P < 0.001$ compared to ctrl using the Mann-Whitney *U* test. *D:* IL-6 and CCL2 levels in supernatants from the same eyes used for flow cytometry were determined by ELISA. Supernatants of 4–6 eyes per group were pooled for one experiment. Data from two independent experiments; Means ± SEM are shown. ***$P < 0.001$ compared to ctrl using the unpaired Student *t*-test. *E.* Representative histology of the mice with and without C4 treatment (n = 5 eyes). Magnification 2× in left panels and 10× in middle and right panels.

2.9. Transwell cell migration assay

Splenocytes (3×10^5 cells/well) were added to the upper wells of microchemotaxis devices (5-μm pore size; 24-well; Transwell; Corning-Costar), and medium with or without RAC culture supernatants was added to the lower wells (Liao et al., 2006). Cells that had migrated to the lower wells after 2 h were collected and counted and analyzed by flow cytometry. The relative chemotaxis was calculated as the ratio of the number of migrated cells in chemoattractant-containing wells divided by the number of migrated cells in medium-containing wells. All

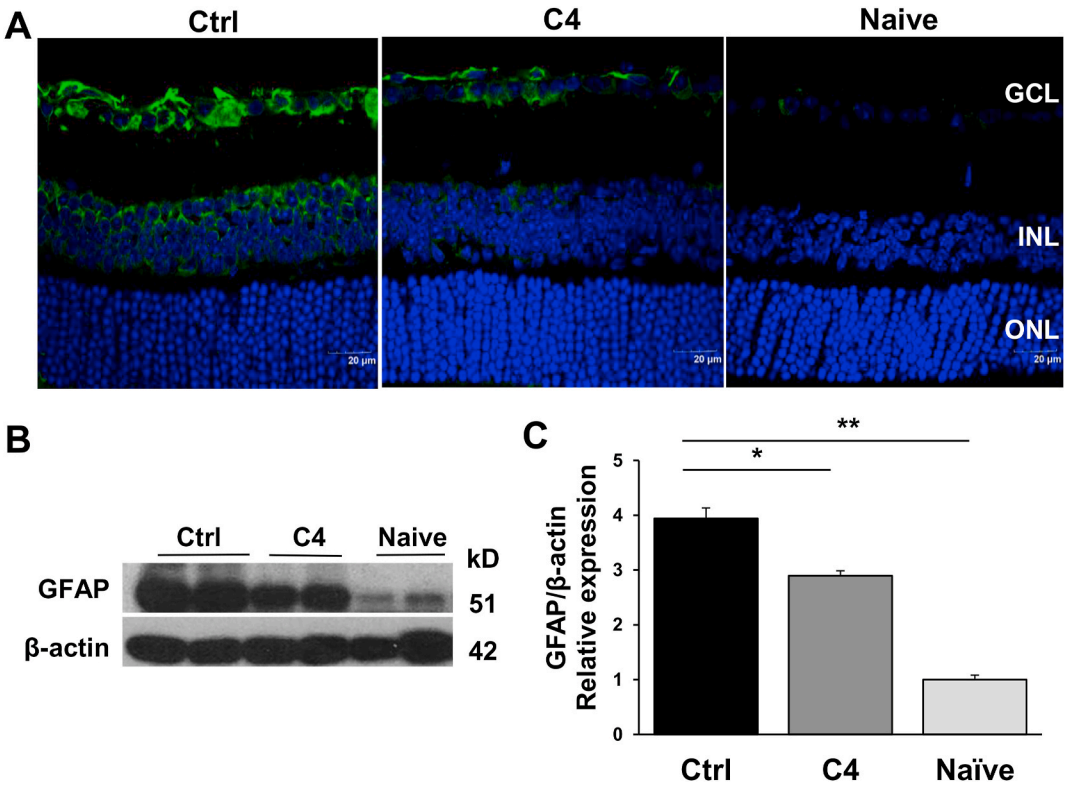

Fig. 3. Treatment of EIU with butyrate (C4) reduced the increased expression of GFAP in the retina.
A: After 18 h of EIU induction, paraffin-embedded sections of retina from naïve mice, EIU mice (ctrl) and EIU with C4 treated mice (n = 5 eyes) were stained with FITC-conjugated anti–GFAP mAb (*green*) and DAPI (*blue for nuclei*) followed by confocal microscopy analysis. Scale bar 20 μm was shown in each panel with 40× magnification. GCL: Ganglion cell layer, INL: Inner nuclear layer; ONL: Outer nuclear layer. B–C: The expression levels of GFAP in the retinas of same mice in A were examined by Western blot. B: Retina lysates were subjected to immunoblot analysis using Abs recognizing GFAP and β-actin. C: The GFAP expression level was expressed as a ratio to β-actin (n = 4 samples). Results represent the means ± S.D of three independent experiments. *p < 0.05. **p < 0.01 using the unpaired Student *t*-test.

assays were performed in triplicate.

2.10. IRBP-specific T cell proliferation and cytokine production following culture of RACs and T cells

The RAC monolayer in 96-well plates was treated with LPS or LPS plus SCFAs for about 20 h, washed out and incubated for 68 h with T cells (4×10^5) isolated from IRBP1-20 immunized B6 (see below) in the presence of IRBP1–20. The culture supernatants were then collected for IFN-γ and IL-17 by ELISA kit (R&D). T cell proliferation was determined using the BrdU assay kit (Roche) from Sigma. The proliferation response was quantified by measuring the optical density (OD) at a wavelength of 450 nm and a reference wavelength of 670 nm using an ELISA reader (Molecular Device) and expressed as mean ± SD of triplicate.

2.11. IRBP1-20 specific T cells for co-culture with RACs

The method to prepare IRBP1-20 specific T cells has been described previously (Jiang et al., 2012). In brief, B6 mice were subcutaneously immunized with human IRBP1–20 (350 μg) and 500 μg *Mycobacterium tuberculosis* H37Ra (Difco, Detroit, MI) in incomplete Freund's adjuvant (Sigma) over six spots on the tail base and flank. Concurrently, 0.2 μg pertussis toxin was intraperitoneally injected. After day 10–13, T cells were isolated from the spleen of immunized mice by passage through a nylon wool column for co-culture with RACs.

2.12. Data analysis

Experiments were performed at least three times. Data were analyzed using the unpaired Student *t*-test and one-way or two-way ANOVA using GraphPad software. Clinical score of EIU was analyzed by Mann-Whitney *U* test. Values determined to be significantly different from those for control or LPS are marked with asterisks in the figures (*$p < 0.05$, **$p < 0.01$).

3. Results

3.1. Both unlabeled and ^{13}C labeled sodium acetate were detected in the eye

Since SCFAs are solely metabolized by gut bacteria (Sun et al., 2017) we ip injected ^{13}C isotopomer labeled precursor of sodium acetate (C2) to determine if it plays a pivotal and direct role in microbiota-gut-eye cross talk. Tissues including the eye, brain and liver were collected from 3 mice after 30 min. Data in Fig. 1 showed that both labeled and unlabeled C2 were detected in each tissue but the peak area of labeled C2 was much lower than unlabeled C2. The ratio of labeled versus unlabeled C2 was stable and highest in the eyes of each mouse compared to the brain and liver.

3.2. SCFAs reduce LPS induced uveitis

To determine whether ip injected SCFAs that enter the eye affect endotoxin-induced uveitis (EIU) in mice, a model resembling acute anterior uveitis in humans, we ip injected B6 mice with 500 mg/kg of butyrate (C4) 30 min prior to intravitreous injection of 250 ng/eye LPS in 1 μL PBS. After 18 h the eyes were clinically evaluated by microcopy (Fig. 2A) and then collected for determining infiltrating inflammatory

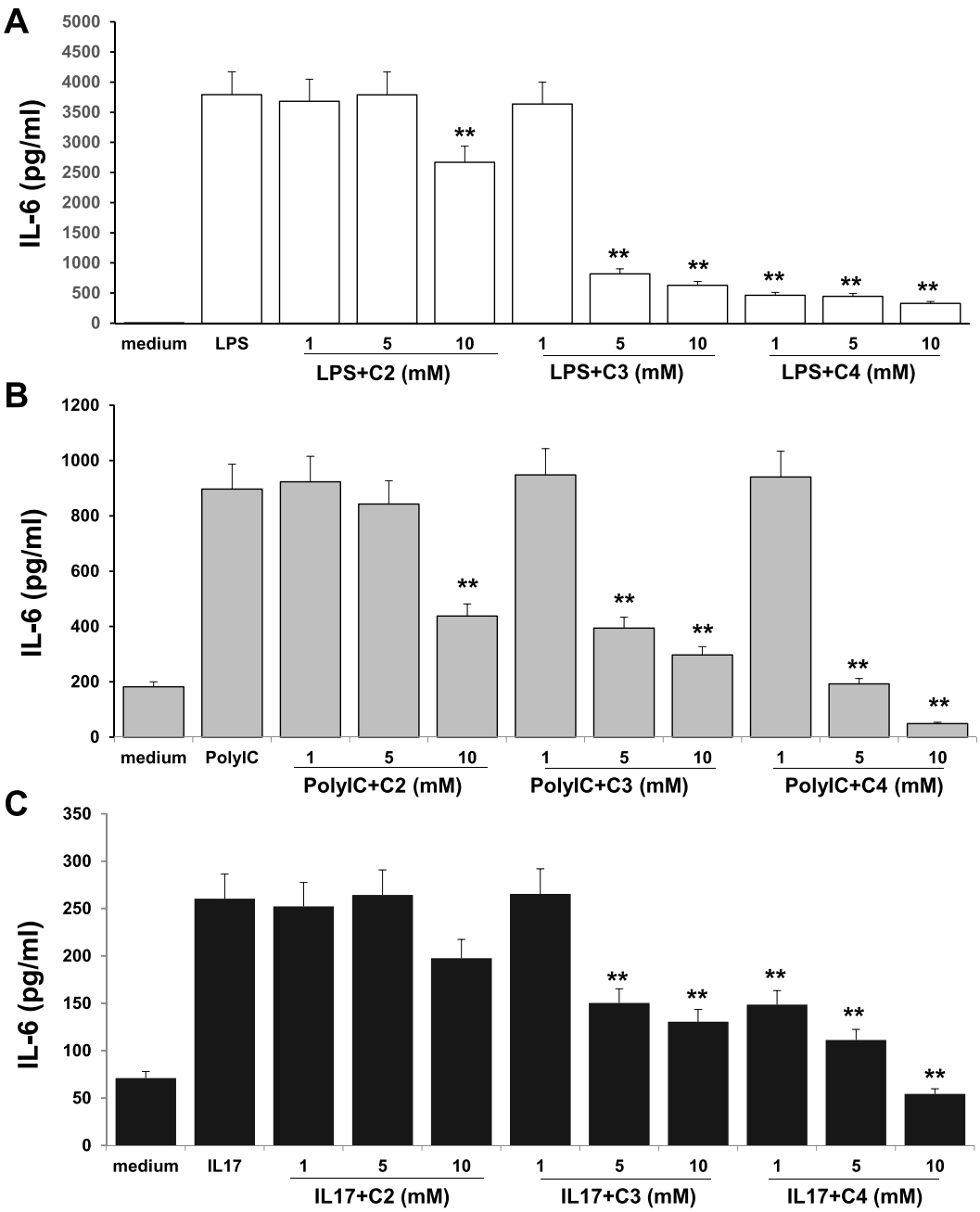

Fig. 4. *SCFAs reduced IL-6 production by RACs in response to LPS, Poly I:C, and IL-17.*
RACs confluent in 24 well plates were incubated in medium alone or medium containing 0.1 μg/ml of LPS (A) or Poly I:C (B), or IL-17 (C) for 20 h in the presence or absence of different doses of SCFAs. SCFAs were added 30 min prior to LPS. The cell supernatants were then collected for testing IL-6 by ELISA. Data are mean ± SD of three independent experiments with triplets in each experiment. *$p < 0.05$ and **$p < 0.01$ compared to the LPS, PolyI:C or IL-17 using the unpaired Student *t*-test.

cells by flow cytometry (Fig. 2B &C), cytokine/chemokines by ELISA (Fig. 2D) and histology (Fig. 2E). We chose 500 mg/kg butyrate based on a previous protocol (Li et al., 2018c). As shown in Fig. 2, clinical signs of ocular inflammation in butyrate (C4) treated mice were significantly milder than control mice (Fig. 2A). Absolute numbers of infiltrating cells ($CD45^+$), and subset of monocytes/macrophages ($CD45^+CD11b^+$ $Ly6c^{hi}$) (Fig. 2B and C) were significantly fewer in the treated group (total 8–12 eyes in each two individual experiments). Moreover, pro-inflammatory cytokines in the pooled AqH, such as IL-6 and CCL2, were significantly reduced in butyrate treated mice (Fig. 2D). Fig. 2 E showed representative histology in EIU, with and without C4 treatment, in which infiltrating inflammatory cells were lower in treated eyes.

3.3. Butyrate (C4) and propionate (C3) reduced the production of IL-6 by RACs in response to LPS, poly I:C and IL-17

Having shown the inhibitory effects of SCFA in EIU in vivo, we further examined whether SCFA affect functions of intraocular resident cells, such as RACs. As seen on confocal microscopy (Fig. 3A) and Western blot (Fig. 3B &C), the expression of GFAP in the retina was greatly increased in mice with EIU compared to naive mice. Treatment with C4 reduced the inflammatory responses of RACs dramatically.

We then isolated RACs to determine the direct effect of SCFAs. We previously reported that RACs produce IL-6 (Jiang et al., 2009; Ke et al., 2009) after exposure to TLRs and cytokines. Therefore, we treated RACs with increasing doses of SCFAs, followed by 0.1 μg/ml of LPS, Poly I:C or

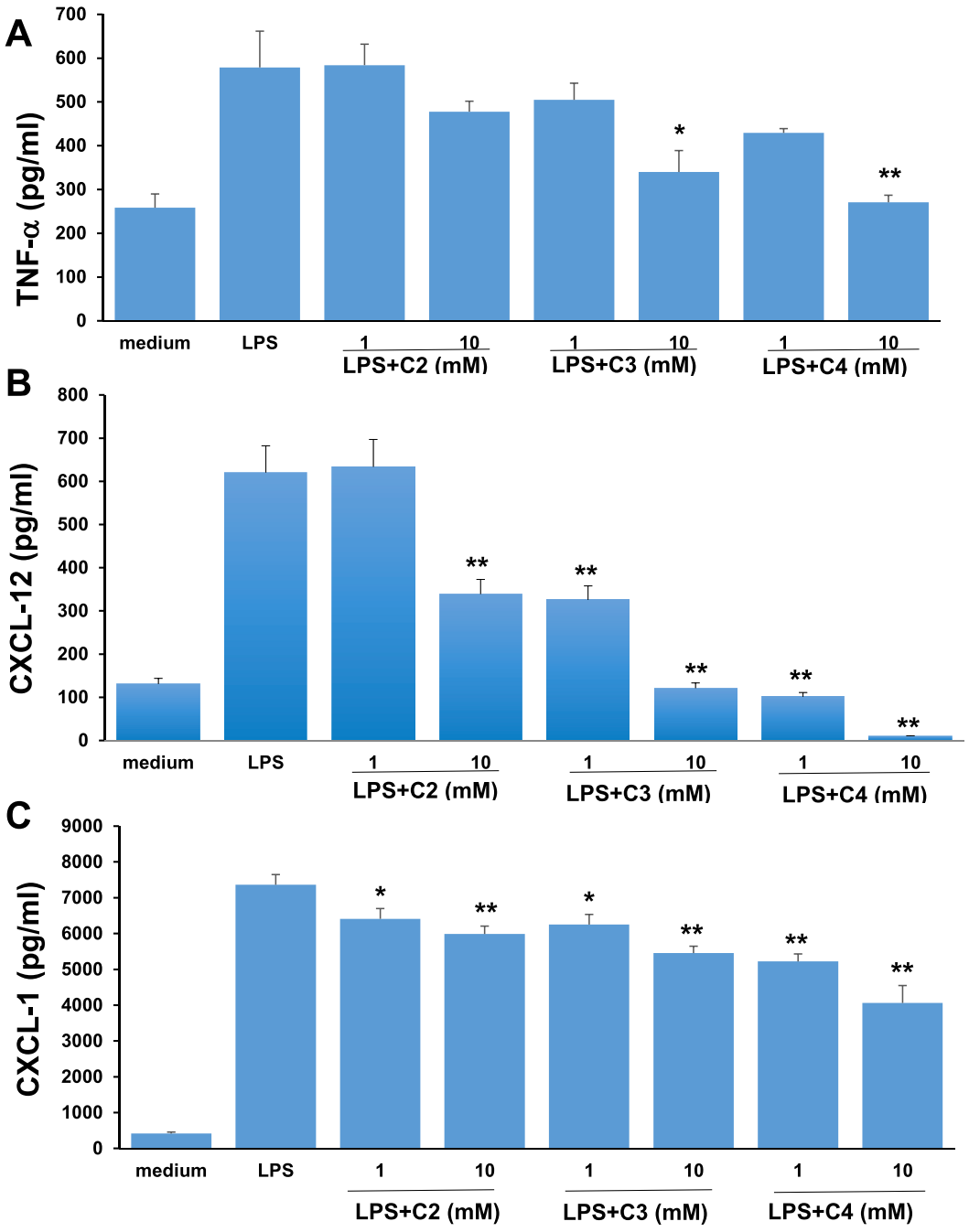

Fig. 5. *SCFAs reduced the production of TNF-α, CXCL12 and CXCL1 by LPS-stimulated RACs.*
The supernatants collected from RAC cultures performed as in Fig. 4A were tested for TNF-α (A), CXCL12 (B) and CXCL1 (C) by ELISA. Data are mean ± SD of three independent experiments. $*p < 0.05$ and $**p < 0.01$ compared to the LPS group using the unpaired Student *t*-test.

IL-17, after which secreted IL-6 levels were measured. As expected, untreated RACs produced very low levels of IL-6; however, RACs treated with LPS, Poly I:C or IL-17 (Fig. 4A–C) released statistically significant increases in IL-6. Importantly, SCFAs inhibited increased IL-6 production in a dose dependent manner, with butyrate (C4) being the most potent inhibitor and acetate (C2) the least. The reduced IL-6 production by RACs upon SCFA treatment was not due to decreased cell proliferation and/or viability. RACs treated up to 48 h with 10 mM acetate, propionate, and butyrate alone or in combination with 0.1 μg/ml of LPS (Supplementary data 1) released a similar amount of LDH, an indicator of cytotoxicity, as the control group.

3.4. SCFAs reduced the production of TNF-α, CXCL12 and CXCL1 by LPS-stimulated RACs

LPS or IL-17 stimulated RACs also produce TNF-α (Jiang et al., 2009; Ke et al., 2009). Moreover, RACs release CXCL12 (Yun et al., 2017) upon encountering HMGB1 or activated uveitogenic T cells, in contrast to LPS stimulated brain astrocytes that release only CXCL1 (Karababa et al., 2017; Liu et al., 2018a). As seen in Fig. 5A–C, LPS-stimulated RACs produced high levels of TNF-α, CXCL12 and CXCL1. However, these levels were markedly reduced by butyrate (C4) and propionate (C3) in a dose dependent manner. Although acetate (C2) did not inhibit TNF-α, it significantly reduced CXCL1 and CXCL12.

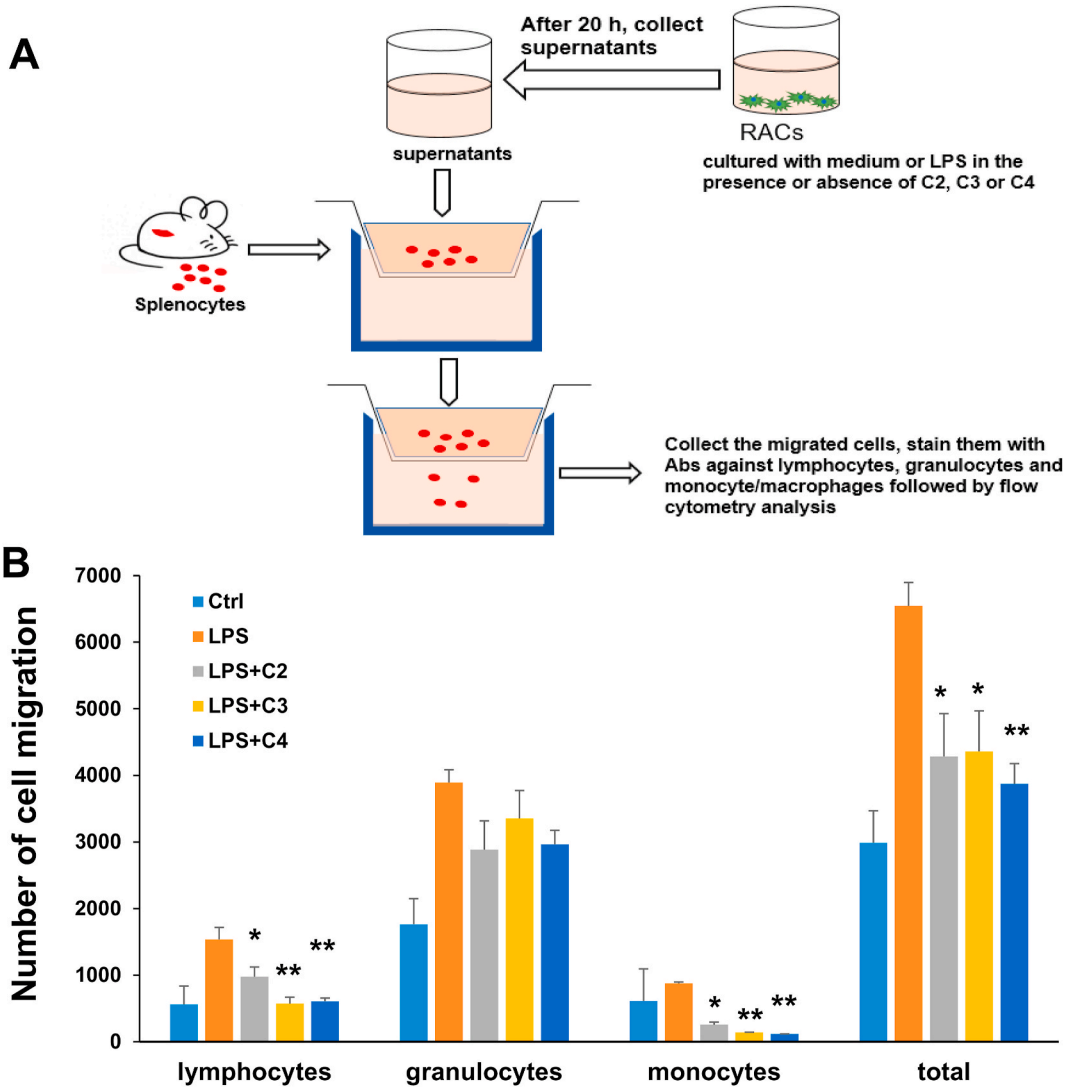

Fig. 6. *SCFAs reduced chemo-attraction of the supernatants of LPS-stimulated RACs.*
A: A diagram of the experimental setting of the immune cell migration assay. Splenocytes (3×10^5 cells/well) were added to the upper wells of microchemotaxis devices. Supernatants collected from RAC cultured with medium or medium containing 0.1 μg/ml LPS in the presence or absence of SCFAs (10 mM C2, 1 mM C3 and C4) were added to the lower wells. Cells that had migrated to the lower wells after 2 h were collected, counted and analyzed by flow cytometry. B. The number of migrated cells. All assays were performed in triplicate. Data are mean ± SD of three independent experiments. *$p < 0.05$ and **$p < 0.01$ compared to the LPS group using the unpaired Student *t*-test.

3.5. SCFAs reduced immune cell migration by LPS-stimulated RACs

We next examined chemoattractive activity in culture supernatants of LPS-stimulated RACs, in the presence or absence of SCFAs, by measuring the migration of lymphocytes, monocytes, granulocytes and total leukocytes. Splenocytes from B6 mice were placed in the top chambers of culture wells separated from the bottom chamber by culture inserts, and the migration of cells to the lower chamber containing different culture supernatants was counted and phenotype determined by FACS analysis (Fig. 6A). As shown in Fig. 6B, significant numbers of leukocytes migrated to the lower chamber of LPS-stimulated RACs in contrast to non-LPS (control) stimulated RACs. However, the increased migration of lymphocytes and monocytes, but not granulocytes, was markedly reduced in the presence of SCFAs in the supernatants. All three SCFAs significantly inhibited the migration of total leukocytes.

3.6. SCFAs promoted IRBP1-20 specific T cell activation

We also investigated the effects of SCFAs on the ability of LPS-stimulated RACs to diminish IRBP-specific T cell proliferation and cytokine production (Jiang et al., 2009). We pre-treated RACs with LPS in the presence or absence of SCFAs for 20 h. We discarded the treatment supernatants and washed the cells thoroughly prior to culture with IRBP-specific T cells and immunizing Ag. These cells were then tested for proliferation using BrdU incorporation and supernatants collected to measure IFN-γ (Th1), IL-17 (Th17) and IL-10 (Treg) levels (Fig. 7). In contrast to the inhibition of C3 and C4 on cytokine/chemokine production of LPS stimulated RACs, these SCFAs increased responder T cell proliferation (Fig. 7A) and production of IFN-γ (Fig. 7C) and IL-17 (Fig. 7E), but not IL-10 (data not shown), lower than but comparable to professional APCs (Fig. 7B, D, F).

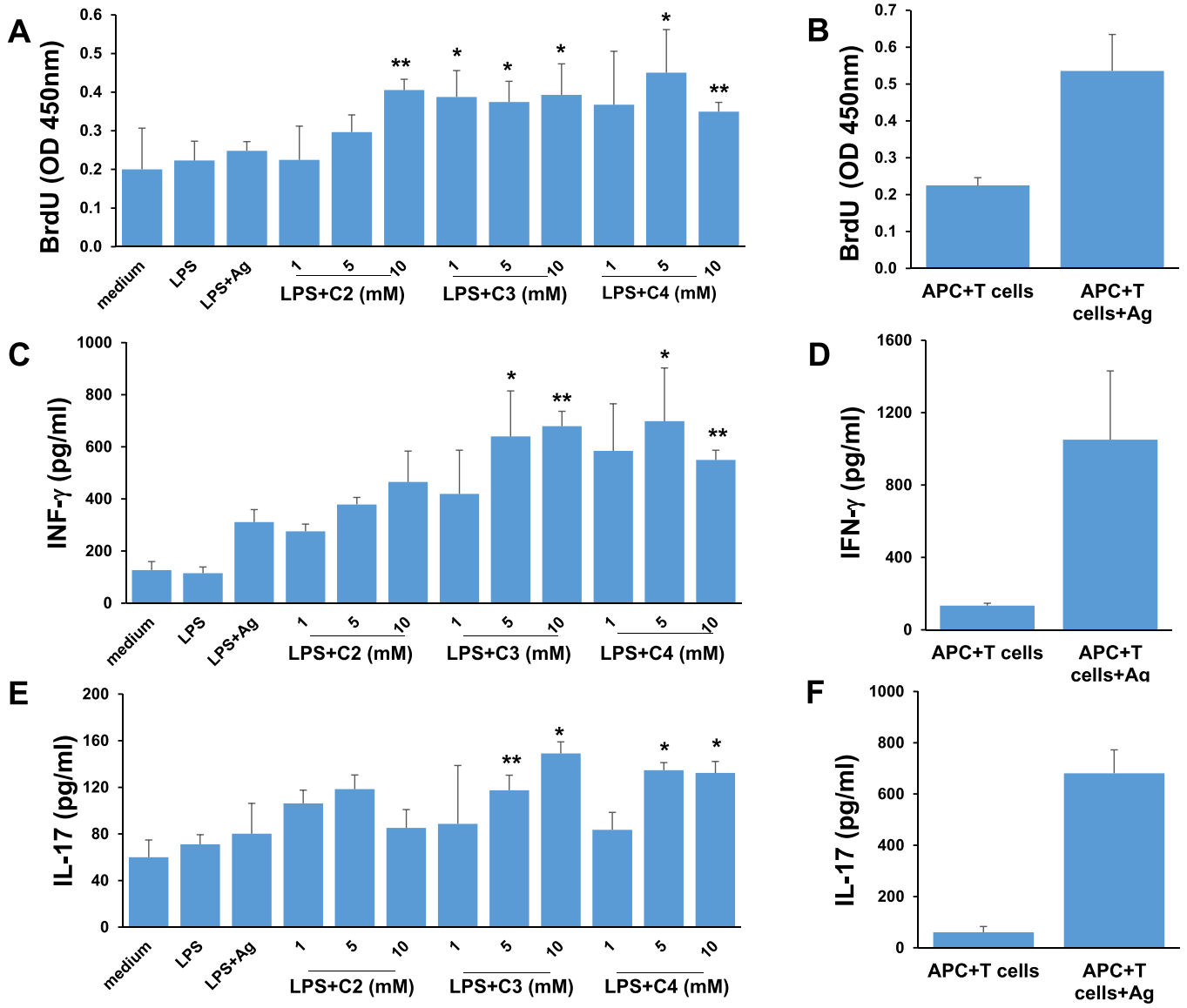

Fig. 7. *C3 and C4 enhanced the proliferation of IRBP-specific T cells and induction of Th1 and Th17 IRBP-specific T cells.*
RACs pre-treated with 0.1 μg/ml of LPS in the presence of C2, C3 or C4 for 20 h were washed to remove LPS and SCFAs before co-cultured with T cells (4×10^5) from IRBP1-20-primed B6 mice and 10 μg/ml IRBP1-20 (A,C and E). Positive control was the same T cells co-cultured with 1×10^5 syngeneic irradiated spleen cells and 10 μg/ml IRBP1-20 (B, D, and F). Proliferation was measured by the incorporation of BrdU during the last 8 h of 68 h incubation period (A-B). The supernatants from triplicate cultures were collected and cytokines measured by ELISA (C–F). Data are mean ± SD of three independent experiments. $^*p < 0.05$ and $^{**}p < 0.01$ compared to the LPS and Ag group using the unpaired Student *t*-test.

3.7. Butyrate (C4) increased the expression of costimulatory molecules on RACs

MHC and costimulatory molecules are required for T-cell activation. Therefore, we studied the expression of these molecules on RACs after exposure to medium, LPS, C2, C4 and combinations of LPS and C2 or C4. After 48 h, the cells were stained with Abs against MHC II and costimulatory molecules CD80, CD86, ICOSL and CD40 and isotype controls. Fig. 8 shows that RAC exposure to LPS and C4 significantly upregulated the expression of MHC class II and costimulatory molecules CD86, ICOSL and CD40.

4. Discussion

The intestinal microbiome plays an important role in the pathogenesis of intraocular inflammation including uveitis (Horai et al., 2015; Janowitz et al., 2019; Nakamura et al., 2016). Drinking of microbiome metabolites such as SCFAs ameliorate immune-mediated uveitis partially by altering migration of lymphocytes from the intestine (Nakamura et al., 2017). Here, we report that a high dose of ip injected SCFAs can reach the eye and inhibit LPS-induced intraocular inflammation. In addition, SCFAs have regulatory effects on RACs. Our observation underscores the importance of the interaction of gut microbiota and their metabolites with the eye, an organ distant from the gut, as well as with a resident intraocular immune regulatory cell, i.e. RACs. Thus, alteration of gut microbiota towards SCFA production or use of supplemental SCFAs may affect the course and severity of intraocular inflammation.

We detected both un-labeled and ^{13}C labeled acetate in the eye. Intraocular unlabeled acetate may be produced in the gut by bacteria and be transported to the eye or be produced by intraocular cells from pyruvate, the product of glycolysis and a key node in the central carbon metabolism of mammalian cells (Liu et al., 2018b). Our data demonstrates that ^{13}C labeled acetate can enter the eye from the bloodstream

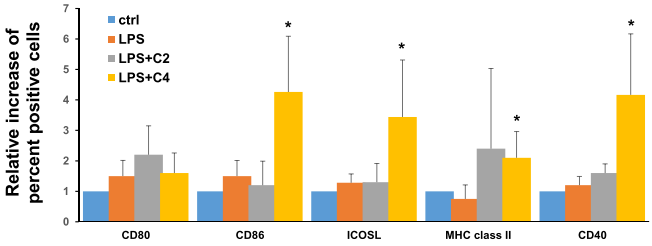

Fig. 8. *C4 increased the expression of MHC class II and co-stimulatory molecule expression on LPS-treated RACs.*
RACs were cultured with 0.1 μg/ml LPS and SCFAs (10 mM C2 and 5 mM C4) as in Fig. 4A. After 48 h, RACs were trypsinized and stained with mAbs against MHC class II, CD80, CD86, ICOSL or CD40 and analyzed by flow cytometry. Negative control samples were stained with isotype-matched control mouse IgG Abs. Relative increase of percent positive cells was calculated as percent positive cells in treatment divided by percent positive in medium in each experiment. Summary of relative increase of percent positive cells (mean ± SD) from four experiments and statistics. $^{*}p < 0.05$ compared to the LPS group using the unpaired Student *t*-test.

and ip injected C4 had an anti-inflammatory effect. Others have also shown the entrance of SCFAs from the circulation into the eye – specifically, isotype labeled valeric acid (VA, C5), another short chain fatty acid, entered the eye following colon injection and decreased intraocular pressure (Skrzypecki et al., 2020); EAU in mice was inhibited by drinking water containing propionate (C3) and butyrate (C4) (Nakamura et al., 2017). These results suggest the existence of gut-eye cross talk and suggest that SCFAs can cross the blood-eye-barrier via the systemic circulation.

Endothelial cells express abundant H-dependent monocarboxylate transporters in the brain that facilitate crossing of the blood brain barrier by SCFAs (Silva et al., 2020). Although we detected high ^{13}C acetate levels in the eye compared to the brain, we do not know the concentration of acetate or the other two SCFAs in ocular tissue. Interestingly, these three SCFAs were present and detectable in human cerebrospinal fluid (http://www.hmdb.ca/) and brain (Bachmann et al., 1979). The physiological concentration of SCFAs in the brain is very low; however, after mice were exposed to live *Clostridium butyricum* the levels of butyrate reached a range from 0.4 to 0.7 μmol/g (Liu et al., 2015), much higher than the concentration in peripheral blood.

Our data demonstrated that ip injected SCFAs reduced not only IL-6 and CCL2, both of which likely contribute to monocyte recruitment in EIU (Chu et al., 2016), but also the inflammatory response of a resident retinal cell, $GFAP^{+}$ RACs. To further dissect the direct role of SCFAs on RACs, we treated isolated RACs with SCFAs and examined their effects. We previously reported that RACs produce multiple cytokines/chemokines such as IL-6, TNF-α and CXCL12 in response to LPS (ligand for TLR4), Poly I:C (ligand for TLR3), bacteria lipoprotein (BLP, ligand for TLR2), muramyl dipeptide (MDP, ligand for NOD2) (Jiang et al., 2009, 2012) and endogenous DAMPs(Yun et al., 2017). We have shown in this study that SCFAs can inhibit IL-6, TNF-α and chemokines CXCL1 and CXCL12 in response to in vitro inflammatory stimuli such as ligands of TLRs and IL-17. In addition, the increased in vitro migration of immune cells by supernatants of LPS stimulated RACs was inhibited by SCFAs. Thus, our in vitro data correlate with our in vivo observations. It should be emphasized that the inhibitory effects of SCFAs on LPS-induced EIU are broad and not just limited to RACs. Furthermore, systemic SCFAs can enter the eye and impact cellular function in the intraocular milieu possibly only at high concentrations.

Butyrate (C4) is the most effective and acetate (C2) the least effective of the SCFAs tested on inhibition of cytokines and chemokines produced by LPS-stimulated RACs. Our culture system (range of SCFA concentrations and exposure to RACs) and results are similar to other cell lines reported in the literature – namely, mouse intestinal epithelial cells (Kim et al., 2013), human vascular endothelial cells(Li et al., 2018a, 2018b), and mouse chondrocytes (Pirozzi et al., 2018). The reduced production of cytokines and chemokines by RACs upon SCFA treatment was not due to decreased cell proliferation and/or viability, since the level of LDH was the same in the culture supernatants of RACs exposed to any tested concentration at 24 h and 48h (supplementary data 1).

We did not study the mechanism by which SCFAs inhibit EIU and regulate LPS-stimulated RACs, but such investigations are underway in our lab. Using an in vitro model, Park et al. demonstrated SCFA-mediated pro- and anti-inflammatory effects through HDAC inhibition (Park et al., 2015). GPCRs, particularly GPR41, GPR43, and GPR109A are receptors for SCFAs and are expressed on immune cells, intestinal epithelial cells, and fatty tissues. Other cell types such as skeletal muscle, smooth muscle and neurons have been recently discovered to express GPR43 and 41 (Ohira et al., 2017). SCFAs can also be absorbed by many cell types and bypass cell-surface receptors to regulate intracellular function.

In addition to the effects of SCFAs on production of cytokines and chemokines by LPS-stimulated RACs, we also examined the effects of SCFAs on antigen presenting functions of RACs. In contrast to the inhibitory effect of SCFAs on cytokine/chemokine production by LPS-RACs, SCFAs enhance the antigen presenting ability of LPS-RACs. When T cells from IRBP1-20 immunized mice were stimulated with IRBP1-20 and LPS-RACs pre-treated with butyrate or propionate, the proliferation of IRBP-specific T cells and the induction of IFN-γ and IL17-producing IRBP-specific T cells were significantly increased. Furthermore, treated RACs expressed increased levels of MHC-II and co-stimulatory molecules CD86, ICOSL and CD40, indicating that butyrate (C4) and propionate (C3) can enhance specific T cell responses without production of IL-12 and IL-23 (data not shown). The model of LPS-induced uveitis represents innate immunity to the endotoxin and not adaptive immunity to a self-antigen. Thus, our in vitro observation that SCFAs may enhance antigen presentation of LPS-RACs to autoimmune T cells is not relevant in this model. Indeed, the effect of SCFAs directly on immune cells including non-professional APCs such as RACs is variable, either enhancing or inhibiting function through activation of GPCR (GPR43, GPR41and GPR109A) or inhibition of HDAC (Sun et al., 2017).

5. Conclusions

Our findings are the first to provide direct evidence of the presence of microbiota-gut-eye crosstalk and demonstrate the inhibitory roles of SCFAs on innate immunity – i.e. cytokines/chemokines from LPS-induced intraocular inflammation and LPS-stimulated RACs. Further studies are necessary to explore whether specific GPCRs and/or HDAC enzymes are involved in the bi-regulatory role of butyrate (C4) and propionate (C3) on RACs. Consequently, altered SCFA levels as a function of diet or microbiota may inhibit or enhance intraocular inflammation depending on the relative effects on innate and adaptive immunity.

Author contributions statement

H.S and H.J.K designed the research. N. C, J. W, J. W, N. P, F. C, T. X, performed the experiments and analyzed the data with advice from H. S.

and Y. Z. H.S, Y.Z. D.S, and H.J.K wrote the manuscript with comments from all other authors.

Supplementary data 1

LDH cell toxicity test. Toxic effects of 10mM acetate, propionate, butyrate and combination of 0.1, 1, 10 mM butyrate and 0.1 μg/ml of LPS at 6 h (A), 24h (B) and 48h (C). Cells treated only with medium were control groups and cells exposed to 1% Triton-X were used as a positive control of cytotoxicity. N=2 times, triplets each times, *p $<$ 0.05 compared with control group using the unpaired Student *t* test.

Declaration of competing interest

The authors declare no competing interests.

Acknowledgement

We thank Dr. Xiang Zhang and Fang Yuan for excellent services in sodium acetate analysis by GC-MS.

This work was supported in part by grant EY024051 from National Institutes of Health (HS), Research to Prevent Blindness (RPB), the Commonwealth of Kentucky Research Challenge Trust Fund, and Sullivan University College of Pharmacy (YZ).

Appendix A. Supplementary data

Supplementary data to this article can be found online at https://doi.org/10.1016/j.exer.2021.108520.

References

Andrade-Oliveira, V., Amano, M.T., Correa-Costa, M., Castoldi, A., Felizardo, R.J., de Almeida, D.C., Bassi, E.J., Moraes-Vieira, P.M., Hiyane, M.I., Rodas, A.C., Peron, J.P., Aguiar, C.F., Reis, M.A., Ribeiro, W.R., Valduga, C.J., Curi, R., Vinolo, M.A., Ferreira, C.M., Camara, N.O., 2015. Gut bacteria products prevent AKI induced by ischemia-reperfusion. J. Am. Soc. Nephrol. : JASN (J. Am. Soc. Nephrol.) 26, 1877–1888.

Bachmann, C., Colombo, J.P., Beruter, J., 1979. Short chain fatty acids in plasma and brain: quantitative determination by gas chromatography. Clin. Chim. Acta; Int. J. Clin. Chem. 92, 153–159.

Chu, C.J., Gardner, P.J., Copland, D.A., Liyanage, S.E., Gonzalez-Cordero, A., Kleine Holthaus, S.M., Luhmann, U.F., Smith, A.J., Ali, R.R., Dick, A.D., 2016. Multimodal analysis of ocular inflammation using the endotoxin-induced uveitis mouse model. Dis. Models Mech. 9, 473–481.

De Majumdar, S., Subinya, M., Korward, J., Pettigrew, A., Scherer, D., Xu, H., 2017. A low concentration of tacrolimus/semifluorinated alkane (SFA) eyedrop suppresses intraocular inflammation in experimental models of uveitis. Curr. Mol. Med. 17, 211–220.

Gardner, P.J., Yazid, S., Ribeiro, J., Ali, R.R., Dick, A.D., 2017. Augmenting endogenous levels of retinal annexin A1 suppresses uveitis in mice. Transl Vis Sci Technol 6, 10.

He, L., Prodhan, M.A.I., Yuan, F., Yin, X., Lorkiewicz, P.K., Wei, X., Feng, W., McClain, C., Zhang, X., 2018. Simultaneous quantification of straight-chain and branched-chain short chain fatty acids by gas chromatography mass spectrometry. J. Chromatogr.. B, Anal. Technol. Biomed. Life Sci. 1092, 359–367.

Horai, R., Zarate-Blades, C.R., Dillenburg-Pilla, P., Chen, J., Kielczewski, J.L., Silver, P. B., Jittayasothorn, Y., Chan, C.C., Yamane, H., Honda, K., Caspi, R.R., 2015. Microbiota-dependent activation of an autoreactive T cell receptor provokes autoimmunity in an immunologically privileged site. Immunity 43, 343–353.

Janowitz, C., Nakamura, Y.K., Metea, C., Gligor, A., Yu, W., Karstens, L., Rosenbaum, J. T., Asquith, M., Lin, P., 2019. Disruption of intestinal homeostasis and intestinal microbiota during experimental autoimmune uveitis. Invest. Ophthalmol. Vis. Sci. 60, 420–429.

Jiang, G., Ke, Y., Sun, D., Han, G., Kaplan, H.J., Shao, H., 2008. Reactivation of uveitogenic T cells by retinal astrocytes derived from experimental autoimmune uveitis-prone B10RIII mice. Invest. Ophthalmol. Vis. Sci. 49, 282–289.

Jiang, G., Ke, Y., Sun, D., Wang, Y., Kaplan, H.J., Shao, H., 2009. Regulatory role of TLR ligands on the activation of autoreactive T cells by retinal astrocytes. Invest. Ophthalmol. Vis. Sci. 50, 4769–4776.

Jiang, G., Sun, D., Kaplan, H.J., Shao, H., 2012. Retinal astrocytes pretreated with NOD2 and TLR2 ligands activate uveitogenic T cells. PloS One 7, e40510.

Jiang, G., Sun, D., Yang, H., Lu, Q., Kaplan, H.J., Shao, H., 2014. HMGB1 is an early and critical mediator in an animal model of uveitis induced by IRBP-specific T cells. J. Leukoc. Biol. 95, 599–607.

Karababa, A., Groos-Sahr, K., Albrecht, U., Keitel, V., Shafigullina, A., Gorg, B., Haussinger, D., 2017. Ammonia attenuates LPS-induced upregulation of pro-inflammatory cytokine mRNA in Co-cultured astrocytes and microglia. Neurochem. Res. 42, 737–749.

Ke, Y., Jiang, G., Sun, D., Kaplan, H.J., Shao, H., 2009. Retinal astrocytes respond to IL-17 differently than retinal pigment epithelial cells. J. Leukoc. Biol. 86, 1377–1384.

Kim, C.H., Park, J., Kim, M., 2014. Gut Microbiota-Derived Short-Chain Fatty Acids, T Cells, and Inflammation, vol. 14. Immune network, pp. 277–288.

Kim, M.H., Kang, S.G., Park, J.H., Yanagisawa, M., Kim, C.H., 2013. Short-chain fatty acids activate GPR41 and GPR43 on intestinal epithelial cells to promote inflammatory responses in mice. Gastroenterology 145, 396–406 e391-310.

Li, M., van Esch, B., Henricks, P.A.J., Folkerts, G., Garssen, J., 2018a. The anti-inflammatory effects of short chain fatty acids on lipopolysaccharide- or tumor necrosis factor alpha-stimulated endothelial cells via activation of GPR41/43 and inhibition of HDACs. Front. Pharmacol. 9, 533.

Li, M., van Esch, B., Henricks, P.A.J., Garssen, J., Folkerts, G., 2018b. Time and concentration dependent effects of short chain fatty acids on lipopolysaccharide- or tumor necrosis factor alpha-induced endothelial activation. Front. Pharmacol. 9, 233.

Li, N., Liu, X.X., Hong, M., Huang, X.Z., Chen, H., Xu, J.H., Wang, C., Zhang, Y.X., Zhong, J.X., Nie, H., Gong, Q., 2018c. Sodium butyrate alleviates LPS-induced acute lung injury in mice via inhibiting HMGB1 release. Int. Immunopharm. 56, 242–248.

Liao, T., Ke, Y., Shao, W.H., Haribabu, B., Kaplan, H.J., Sun, D., Shao, H., 2006. Blockade of the interaction of leukotriene b4 with its receptor prevents development of autoimmune uveitis. Invest. Ophthalmol. Vis. Sci. 47, 1543–1549.

Liu, J., Sun, J., Wang, F., Yu, X., Ling, Z., Li, H., Zhang, H., Jin, J., Chen, W., Pang, M., Yu, J., He, Y., Xu, J., 2015. Neuroprotective effects of Clostridium butyricum against vascular dementia in mice via metabolic butyrate. BioMed Res. Int. 2015, 412946.

Liu, S., Lu, C., Liu, Y., Zhou, X., Sun, L., Gu, Q., Shen, G., Guo, A., 2018a. Hyperbaric oxygen alleviates the inflammatory response induced by LPS through inhibition of NF-kappaB/MAPKs-CCL2/CXCL1 signaling pathway in cultured astrocytes. Inflammation 41, 2003–2011.

Liu, X., Cooper, D.E., Cluntun, A.A., Warmoes, M.O., Zhao, S., Reid, M.A., Liu, J., Lund, P.J., Lopes, M., Garcia, B.A., Wellen, K.E., Kirsch, D.G., Locasale, J.W., 2018b. Acetate production from glucose and coupling to mitochondrial metabolism in mammals. Cell 175, 502–513 e513.

Lozano, D.C., Choe, T.E., Cepurna, W.O., Morrison, J.C., Johnson, E.C., 2019. Early optic nerve head glial proliferation and jak-stat pathway activation in chronic experimental glaucoma. Invest. Ophthalmol. Vis. Sci. 60, 921–932.

Ly, A., Yee, P., Vessey, K.A., Phipps, J.A., Jobling, A.I., Fletcher, E.L., 2011. Early inner retinal astrocyte dysfunction during diabetes and development of hypoxia, retinal stress, and neuronal functional loss. Invest. Ophthalmol. Vis. Sci. 52, 9316–9326.

Matt, S.M., Allen, J.M., Lawson, M.A., Mailing, L.J., Woods, J.A., Johnson, R.W., 2018. Butyrate and dietary soluble fiber improve neuroinflammation associated with aging in mice. Front. Immunol. 9, 1832.

Nakamura, Y.K., Janowitz, C., Metea, C., Asquith, M., Karstens, L., Rosenbaum, J.T., Lin, P., 2017. Short chain fatty acids ameliorate immune-mediated uveitis partially by altering migration of lymphocytes from the intestine. Sci. Rep. 7, 11745.

Nakamura, Y.K., Metea, C., Karstens, L., Asquith, M., Gruner, H., Moscibrocki, C., Lee, I., Brislawn, C.J., Jansson, J.K., Rosenbaum, J.T., Lin, P., 2016. Gut microbial alterations associated with protection from autoimmune uveitis. Invest. Ophthalmol. Vis. Sci. 57, 3747–3758.

Ohira, H., Tsutsui, W., Fujioka, Y., 2017. Are short chain fatty acids in gut microbiota defensive players for inflammation and atherosclerosis? J. Atherosclerosis Thromb. 24, 660–672.

Park, J., Kim, M., Kang, S.G., Jannasch, A.H., Cooper, B., Patterson, J., Kim, C.H., 2015. Short-chain fatty acids induce both effector and regulatory T cells by suppression of histone deacetylases and regulation of the mTOR-S6K pathway. Mucosal Immunol. 8, 80–93.

Pirozzi, C., Francisco, V., Guida, F.D., Gomez, R., Lago, F., Pino, J., Meli, R., Gualillo, O., 2018. Butyrate modulates inflammation in chondrocytes via GPR43 receptor. Cell. Physiol. Biochem. : Int. J. Exp. Cell. Physiol. Biochem. Pharm. 51, 228–243.

Qiu, Y., Shil, P.K., Zhu, P., Yang, H., Verma, A., Lei, B., Li, Q., 2014. Angiotensin-converting enzyme 2 (ACE2) activator diminazene aceturate ameliorates endotoxin-induced uveitis in mice. Invest. Ophthalmol. Vis. Sci. 55, 3809–3818.

Ramirez, J.M., Ramirez, A.I., Salazar, J.J., de Hoz, R., Trivino, A., 2001. Changes of astrocytes in retinal ageing and age-related macular degeneration. Exp. Eye Res. 73, 601–615.

Rosenbaum, J.T., Woods, A., Kezic, J., Planck, S.R., Rosenzweig, H.L., 2011. Contrasting ocular effects of local versus systemic endotoxin. Invest. Ophthalmol. Vis. Sci. 52, 6472–6477.

Selvam, S., Kumar, T., Fruttiger, M., 2018. Retinal vasculature development in health and disease. Prog. Retin. Eye Res. 63, 1–19.

Silva, Y.P., Bernardi, A., Frozza, R.L., 2020. The role of short-chain fatty acids from gut microbiota in gut-brain communication. Front. Endocrinol. 11, 25.

Skrzypecki, J., Nieweglowska, K., Samborowska, E., 2020. Valeric acid, a gut microbiota product, penetrates to the eye and lowers intraocular pressure in rats. Nutrients 12.

Slavi, N., Toychiev, A.H., Kosmidis, S., Ackert, J., Bloomfield, S.A., Wulff, H., Viswanathan, S., Lampe, P.D., Srinivas, M., 2018. Suppression of connexin 43 phosphorylation promotes astrocyte survival and vascular regeneration in proliferative retinopathy. Proc. Natl. Acad. Sci. U. S. A. 115, E5934–E5943.

Sun, M., Wu, W., Liu, Z., Cong, Y., 2017. Microbiota metabolite short chain fatty acids, GPCR, and inflammatory bowel diseases. J. Gastroenterol. 52, 1–8.

Theiler, A., Barnthaler, T., Platzer, W., Richtig, G., Peinhaupt, M., Rittchen, S., Kargl, J., Ulven, T., Marsh, L.M., Marsche, G., Schuligoi, R., Sturm, E.M., Heinemann, A.,

2019. Butyrate ameliorates allergic airway inflammation by limiting eosinophil trafficking and survival. J. Allergy Clin. Immunol. 144, 764–776.
Williams, P.A., Marsh-Armstrong, N., Howell, G.R., Lasker, I.I.o.A., Glaucomatous Neurodegeneration, P., 2017. Neuroinflammation in glaucoma: a new opportunity. Exp. Eye Res. 157, 20–27.
Yun, J., Jiang, G., Wang, Y., Xiao, T., Zhao, Y., Sun, D., Kaplan, H.J., Shao, H., 2017. The HMGB1-CXCL12 complex promotes inflammatory cell infiltration in uveitogenic T cell-induced chronic experimental autoimmune uveitis. Front. Immunol. 8, 142.